5

Ground-state properties of nuclei: the shell model

5.1 Nuclear potential wells

In the last chapter, we set out a semi-empirical theory for the binding energy of an atomic nucleus, and quantum-mechanical considerations came in only rather indirectly. Experimental atomic masses show deviations from the smooth curve given by the semi-empirical mass formula, deviations which we said were of quantum-mechanical origin. Since a nucleus in its ground state is a quantum system of finite size, it has angular momentum $\mathbf{J}$, with quantum number j which is some integral multiple of $\frac{1}{2}$. If $j \neq 0$ the nucleus will have a magnetic dipole moment, and it may have an electric quadrupole moment as well.

The nuclear angular momentum and magnetic moment manifest themselves most immediately in atomic spectroscopy, where the interaction between the nuclear magnetic moment and the electron magnetic moments gives rise to the hyperfine structures of the electronic energy levels. In favourable cases both j and the magnetic moment may be deduced from this hyperfine splitting.

The observed values of nuclear angular momenta give strong support to the validity of a simple quantum-mechanical model of the nucleus: the nuclear shell model. In this model, each neutron moves independently in a common potential well that is the spherical average of the nuclear potential produced by all the other nucleons, and each proton moves independently in a common potential well that is the spherical average of the nuclear potential of all the other nucleons, together with the Coulomb potential of the other protons. Since the nuclear forces are of short range we can guess that the shape of such an average nuclear potential will

https://doi.org/10.1017/CBO9781139164405.008 Published online by Cambridge University Press

reflect the nuclear density exhibited in Fig. 4.4. In particular it will be uniform in the central region and rise steeply in the surface region. Indeed, we can anticipate that the steep rise will be even more pronounced than the fall in nuclear density, since tunnelling into the classically forbidden region will make the nuclear density near the surface more diffuse. Thus the potential wells for neutrons and protons will be, qualitatively, as sketched in Fig. 5.1(*a*) and Fig. 5.1(*b*).

In order to model the effect of proton charge, we have added to the proton well the Coulomb potential energy $U_c(r)$ of a proton in a sphere of uniform charge density and total charge $(Z-1)e$, corresponding to a uniform distribution of the other $(Z-1)$ protons. (Such a charge distribution gave an energy which agreed well with the empirical Coulomb contribution in the mass formula.) Elementary electrostatics gives

$$U_c(r) = \begin{cases} \dfrac{(Z-1)e^2}{4\pi\varepsilon_0 R}\left[\dfrac{3}{2} - \dfrac{r^2}{2R^2}\right], & r < R, \\ \dfrac{(Z-1)e^2}{4\pi\varepsilon_0 r}, & r > R, \end{cases} \tag{5.1}$$

where R is the nuclear radius.

Since the basic nucleon–nucleon interaction is state-dependent, there are other factors which affect the relative depths of the neutron and proton wells. For nuclei with more neutrons than protons the contribution of the strong nucleon–nucleon interaction to the potential is more

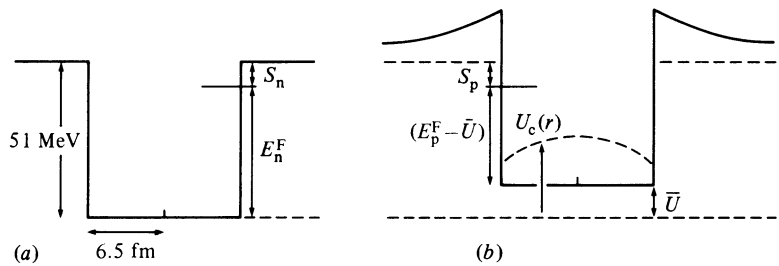


Fig. 5.1 A schematic representation of (*a*) the neutron potential well and (*b*) the proton potential well for the nucleus $^{208}_{82}$Pb. E_n^F and $(E_P^F - \bar{U})$ have been estimated using equation (5.5). The observed neutron separation energy S_n of 7.4 MeV implies a neutron well-depth of 51 MeV. The observed proton separation energy S_p of 8.9 MeV implies that $\bar{U} = 11$ MeV. $\bar{U}$ represents the sum of the mean electrostatic potential and the asymmetry energy.

https://doi.org/10.1017/CBO9781139164405.008 Published online by Cambridge University Press

attractive for the protons than for the neutrons, since a proton in such a nucleus is, on average, more subject to the neutron–proton interaction (recall the discussion of symmetry energy in §4.5). This lowers the proton well-depth relative to $U_c(r)$, as is indicated in Fig. 5.1(*b*) (which is drawn with parameters appropriate to $^{208}_{82}$Pb). The nuclear shell model treats all these effects empirically.

5.2 Estimates of nucleon energies

Let us, for the moment, disregard the details of the nuclear potential at the surface, and replace it by a potential with infinitely high walls at $r = R$, which force the nucleon wave-functions to be zero at, and outside, $r = R$. We measure energies from the bottom of the neutron well, and for simplicity take the proton well to be raised with respect to the neutron well by a constant energy $\bar{U}$. This $\bar{U}$ represents the mean electrostatic potential and any asymmetry contributions to the proton potential well. Then the Schrödinger equations for the neutron states ψ_n and proton states ψ_p are respectively

$$-\frac{\hbar^2}{2m_n}\nabla^2\psi_n = E_n\psi_n, \tag{5.2}$$

$$-\frac{\hbar^2}{2m_p}\nabla^2\psi_p = (E_p - \bar{U})\psi_p, \tag{5.3}$$

where any terms involving the intrinsic spin of the nucleons have been neglected.

Nucleons are fermions, and the Pauli exclusion principle requires that no two neutrons nor two protons are in the same state. Hence in the shell model of the ground state of a nucleus with N neutrons and Z protons, the lowest N neutron states are occupied up to some energy E_n^F, called the neutron Fermi energy, and the lowest Z proton states are occupied up to some energy E_p^F, the proton Fermi energy. To obtain a qualitative estimate of the energies involved, we suppose that N and Z are sufficiently large for us to use the elementary formula for the integrated density of states $\mathcal{N}(E)$, derived in Appendix B,

$$\mathcal{N}(E) = \frac{V}{3\pi^2}\left(\frac{2mE}{\hbar^2}\right)^{\frac{3}{2}}, \tag{5.4}$$

https://doi.org/10.1017/CBO9781139164405.008 Published online by Cambridge University Press

where V is the volume of the system considered, in this case the nuclear volume $V = 4\pi R^3/3$. Hence E_n^F and E_p^F are given by

$$N \approx \frac{V}{3\pi^2}\left(\frac{2m_n E_n^F}{\hbar^2}\right)^{\frac{3}{2}}, \quad Z \approx \frac{V}{3\pi^2}\left(\frac{2m_p(E_p^F - \bar{U})}{\hbar^2}\right)^{\frac{3}{2}}, \tag{5.5}$$

since proton kinetic energies are given by $(E_p - \bar{U})$.

In lighter nuclei, $A \lesssim 40$, the number of neutrons and protons is approximately equal, so that N/V is close to half the 'density of nuclear matter' given by equation (4.2), i.e. $N/V \approx 0.085\ \mathrm{fm}^{-3}$. For this density, equation (5.5) gives $E_n^F \approx 38$ MeV, irrespective of the particular nucleus. For heavier nuclei, this figure will increase somewhat, but for energies of this order the corresponding neutron velocities are quite low: $v_F^2/c^2 \approx 0.1$. This gives some justification for our use of the non-relativistic Schrödinger equation for the neutrons. Similarly, a proton at the Fermi energy E_p^F has kinetic energy $(E_p^F - \bar{U}) \approx 38$ MeV also.

Similar energies are to be expected in more realistic potentials of finite depth. In a finite well, the depth of E_n^F below the external potential outside the nucleus is equal to the energy required to detach a neutron from the nucleus. This energy, the *neutron separation energy* S_n, is given in terms of binding energies by

$$S_n(N, Z) = B(N, Z) - B(N - 1, Z), \tag{5.6}$$

and hence is of the order of the binding energy per nucleon, about 8 MeV (Fig. 4.7, see also Table 4.2). Thus the total depth of the neutron well is ≈ 46 MeV.

Similarly the proton separation energy is defined by

$$S_p(N, Z) = B(N, Z) - B(N, Z - 1).$$

The most stable nucleus of a given mass number $A = N + Z$ will have the neutron and proton Fermi energies approximately equal: if they were to differ in energy by more than $\sim(m_e c^2 +$ energy level spacing), the nucleus would be unstable to β-decay. A nucleon at the higher Fermi energy would decay to an empty state just above the lower Fermi energy, to form a new nucleus with different charge, and lower total energy. An equivalent condition is that S_n and S_p must be approximately equal.

The characteristic velocity of a nucleon at the Fermi energy, and the radius R of the nucleus, set a typical *nuclear time scale* t_{nuc}:

https://doi.org/10.1017/CBO9781139164405.008 Published online by Cambridge University Press

$$t_{\text{nuc}} = \frac{2R}{v_{\text{F}}} \approx 2.6 \times 10^{-23} \times A^{\frac{1}{3}} \text{ s}. \tag{5.7}$$

5.3 Energy shells and angular momentum

To obtain more precise information about the nucleon levels we must solve the Schrödinger equations (5.2) and (5.3). For simplicity, we again take the potential wells with infinite walls. The Schrödinger equations are separable in (r, θ, ϕ) coordinates so that

$$\psi(r, \theta, \phi) = u_l(r) Y_{lm}(\theta, \phi),$$

where $l = 0, 1, 2, 3, \ldots$ and $m = -l, -l+1, \ldots, l-1, l$, are orbital angular momentum quantum numbers (Appendix C). States with $l = 0, 1, 2, 3, 4, 5, \ldots$ are called s, p, d, f, g, h, … states, the notation having been established in the early days of atomic spectroscopy. Taking equation (5.2) for neutrons (and the equation for protons differs only in the shift $\bar{U}$ in energy), the radial function $u_l(r)$ satisfies

$$\frac{-\hbar^2}{2m_{\text{n}}} \frac{1}{r} \frac{\mathrm{d}^2}{\mathrm{d}r^2}(ru_l) + \frac{\hbar}{2m_{\text{n}}} \frac{l(l+1)}{r^2} u_l = E u_l, \tag{5.8}$$

with the boundary conditions that $u(r)$ is finite at $r = 0$ and zero at $r = R$.

When $l = 0$ (s-states) we see immediately that the solutions finite at $r = 0$ are

$$u_{\text{s}}(r) = \frac{\sin(kr)}{kr} \quad \text{with } E = \frac{\hbar^2 k^2}{2m_{\text{n}}}. \tag{5.9}$$

The boundary condition at $r = R$ is satisfied by taking $k = k_n = n\pi/R$, where $n = 1, 2, 3, \ldots$, and the corresponding energy levels 1s, 2s, 3s, …, are given by

$$E(n, s) = \frac{\hbar^2}{2m_{\text{n}}} \left(\frac{n\pi}{R}\right)^2. \tag{5.10}$$

Thus there is a sequence of energy eigenstates having $l = 0$, labelled by the additional quantum number n. When $l = 1$ (p-states) the Schrödinger equation is

https://doi.org/10.1017/CBO9781139164405.008 Published online by Cambridge University Press

$$-\frac{\hbar^2}{2m_\mathrm{n}}\frac{1}{r}\frac{\mathrm{d}^2}{\mathrm{d}r^2}(ru_\mathrm{p})+\frac{\hbar^2}{m_\mathrm{n}r^2}u_\mathrm{p}=Eu_\mathrm{p}, \tag{5.11}$$

and it is straightforward to check by differentiation that the solution finite at $r=0$ is

$$u_\mathrm{p}(r)=\frac{\sin(kr)}{(kr)^2}-\frac{\cos(kr)}{(kr)}, \qquad E=\frac{\hbar^2}{2m_\mathrm{n}}k^2. \tag{5.12}$$

We must again choose k so that $u_\mathrm{p}(R)=0$. Let us write $kR=x$. The values of x for which $u_\mathrm{p}(R)=0$ are $x_{1\mathrm{p}}=4.49$, $x_{2\mathrm{p}}=7.73,\ldots$, and the corresponding energies are $E(n,p)=(\hbar^2/2m_\mathrm{n})(x_{\mathrm{np}}/R)^2$. It should be noted that the labelling of energy levels, $n=1,2,3,\ldots$, for each l value, differs from that conventionally adopted in atomic physics.

In fact $u_\mathrm{s}(r)$ and $u_\mathrm{p}(r)$ are special cases of the *spherical Bessel functions* $j_l(kr)$. For arbitrary l the zeros of $j_l(x)$, which give the allowed values of k, are tabulated in standard tables of mathematical functions, and given in column (2) of Table 5.1. Thus for any l the levels $E(n,l)=(\hbar^2/2m)(x_{\mathrm{n}l}/R)^2$ are easily determined, and hence their sequence in order of increasing energy. This is given in columns (1) and (7) of Table 5.1. For each $E(n,l)$, there are $(2l+1)$ allowed values of the quantum number m. Since we have so far neglected any coupling between the intrinsic spin of a nucleon and its orbital motion, each nucleon has two possible spin states, which may be characterised by $m_\mathrm{s}=\frac{1}{2}, m_\mathrm{s}=-\frac{1}{2}$, so that there are $(4l+2)$ states of the same energy for a given (n,l).

The sequence of the levels $E(n,l)$ is not very sensitive to the precise details of the well, and is much the same for a well of finite depth and appropriately rounded shape. If N neutrons are put into the neutron well, the ground state (which may be degenerate) will correspond to the occupation of the N lowest lying energy states. Figure 5.2 expresses graphically the number of states available in terms of the dimensionless quantity $x=kR$. $\mathcal{N}(x)$ is the number of states with energy less than $(\hbar^2/2m_\mathrm{n})(x/R)^2$ or, equivalently, the number of zeros x_{nl} with $x_{nl}<x$, each zero being counted $(4l+2)$ times. Also drawn is the asymptotic formula, valid for large x,

$$\mathcal{N}(x)=\frac{4x^3}{9\pi}\left(1-\frac{9\pi}{8x}\right)=\frac{V}{3\pi^2}\left(\frac{2m_\mathrm{n}E}{\hbar^2}\right)^{\frac{3}{2}}\left[1-\frac{3\pi}{8}\frac{S}{V}\left(\frac{\hbar^2}{2m_\mathrm{n}E}\right)^{\frac{1}{2}}\right]. \tag{5.13}$$

https://doi.org/10.1017/CBO9781139164405.008 Published online by Cambridge University Press

Table 5.1

	x_{nl}	Neutron		Proton		
1s	3.14	$1s_{\frac{1}{2}}$	2	2	$1s_{\frac{1}{2}}$	1s
1p	4.49	$1p_{\frac{3}{2}}$	6	6	$1p_{\frac{3}{2}}$	1p
		$1p_{\frac{1}{2}}$	8	8	$1p_{\frac{1}{2}}$	
1d	5.76	$1d_{\frac{5}{2}}$	14	14	$1d_{\frac{5}{2}}$	1d
		$2s_{\frac{1}{2}}$	16	16	$2s_{\frac{1}{2}}$	
2s	6.28	$1d_{\frac{3}{2}}$	20			2s
				20	$1d_{\frac{3}{2}}$	
1f	6.99	$1f_{\frac{7}{2}}$	28			
		$2p_{\frac{3}{2}}$	32	28	$1f_{\frac{7}{2}}$	
2p	7.73	$1f_{\frac{5}{2}}$	38			1f
		$2p_{\frac{1}{2}}$	40	32	$2p_{\frac{3}{2}}$	
1g	8.18	$1g_{\frac{9}{2}}$	50	38	$1f_{\frac{5}{2}}$	2p
		$2d_{\frac{5}{2}}$	56	40	$2p_{\frac{1}{2}}$	
2d	9.10	$1g_{\frac{7}{2}}$	64			
		$1h_{\frac{11}{2}}$	76	50	$1g_{\frac{9}{2}}$	
1h	9.36	$3s_{\frac{1}{2}}$	78			1g
		$2d_{\frac{3}{2}}$	82	58	$1g_{\frac{7}{2}}$	
3s	9.42	$2f_{\frac{7}{2}}$	90	64	$2d_{\frac{5}{2}}$	
		$1h_{\frac{9}{2}}$	100			
2f	10.42	$3p_{\frac{3}{2}}$	104			2d
1i	10.51	$1i_{\frac{13}{2}}$	118	76	$1h_{\frac{11}{2}}$	
		$2f_{\frac{5}{2}}$	124	80	$2d_{\frac{3}{2}}$	1h
3p	10.90	$3p_{\frac{1}{2}}$	126	82	$3s_{\frac{1}{2}}$	
						3s
		$2g_{\frac{9}{2}}$	136			
1j	11.66	$1i_{\frac{11}{2}}$	148	92	$1h_{\frac{9}{2}}$	
		$2g_{\frac{7}{2}}$	156	100	$2f_{\frac{7}{2}}$	
2g	11.70					

The first and last columns give the sequence of energy levels in a spherical well with infinite walls. The second column gives the corresponding values of $x_{nl} = k_{nl}R$. The third column gives the observed sequence of spin–orbit coupled levels for neutrons, and the fourth the cumulative number of available states in these levels. The remaining two columns give the levels and number of states for protons. The spacings are chosen so that the filling of the neutron and proton shells for stable nuclei is approximately in step down the columns. Lines are drawn at the 'magic numbers'.

https://doi.org/10.1017/CBO9781139164405.008 Published online by Cambridge University Press

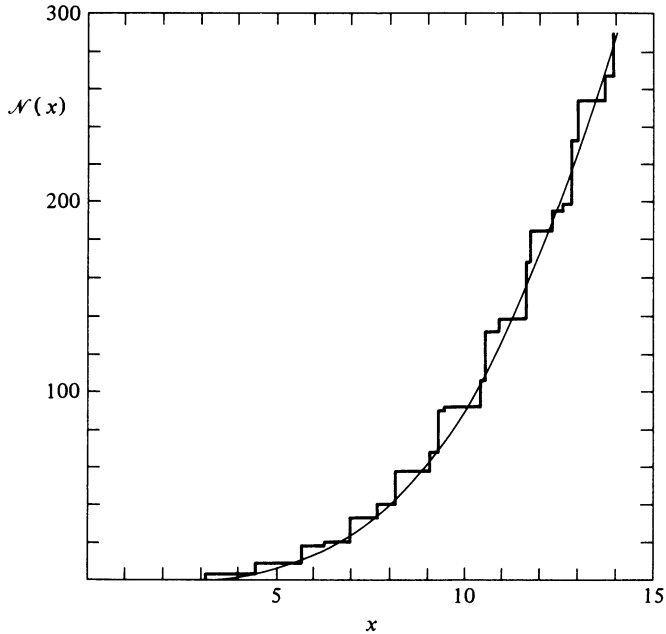


Fig. 5.2 The exact $\mathcal{N}(x)$ compared with the asymptotic formula of equation (5.13). (See Baltes, H. P. and Hilf, E. R. (1976), *Spectra of Finite Systems*, for the derivation of (5.13).)

This is an extension of the usual density of states formula we used in equation (5.4) and includes a correction for the effects of the surface (of area S). It follows the exact $\mathcal{N}(x)$ remarkably closely.

So far we have neglected spin. The crucial step in establishing the nuclear shell model was the recognition that there must also be a *spin–orbit coupling* term in the self-consistent potential seen by the nucleons, of the form

$$U_{\mathrm{so}}(r)\mathbf{L}\cdot\mathbf{s}. \tag{5.14}$$

A term like this is not perhaps too surprising since in the basic nucleon–nucleon interaction, equation (3.4), there is coupling between the spins and the orbital motions of the nucleons.

With the introduction of this spin–orbit coupling term into the potential, $\mathbf{L}^2$ and $\mathbf{s}^2$ are still conserved since

$$[\mathbf{L}^2, \mathbf{L}\cdot\mathbf{s}] = 0, \quad [\mathbf{s}^2, \mathbf{L}\cdot\mathbf{s}] = 0, \tag{5.15}$$

https://doi.org/10.1017/CBO9781139164405.008 Published online by Cambridge University Press

so that l and $s(=\frac{1}{2})$ remain good quantum numbers, but m and m_s, are 'good quantum numbers' no longer, since

$$[L_z, \mathbf{L}\cdot\mathbf{s}] \neq 0, \quad [m_s, \mathbf{L}\cdot\mathbf{s}] \neq 0. \tag{5.16}$$

Thus the magnitudes, but not the directions, of $\mathbf{L}$ and $\mathbf{s}$ are preserved. However, the *total angular momentum* $\mathbf{J} = \mathbf{L} + \mathbf{s}$ is of course conserved, so that states may be specified by the quantum numbers (l, s, j, j_z). In Appendix C it is shown that for a given l and $s = \frac{1}{2}$, the allowed values of j are: $l + \frac{1}{2}$, with $[2(l + \frac{1}{2}) + 1] = 2l + 2$ allowed values of j_z; and $l - \frac{1}{2}$, with $[2(l - \frac{1}{2}) + 1] = 2l$ allowed values of j_z. The parity of the state specified by $(l, s, l \pm \frac{1}{2}, j_z)$ is $(-1)^l$.

The expectation value of $\mathbf{L}\cdot\mathbf{s}$ may be obtained from the identity

$$\mathbf{L}\cdot\mathbf{s} = \tfrac{1}{2}[(\mathbf{L}+\mathbf{s})^2 - \mathbf{L}^2 - \mathbf{s}^2] = \tfrac{1}{2}[\mathbf{J}^2 - \mathbf{L}^2 - \mathbf{s}^2], \tag{5.17}$$

so that

$$\begin{aligned}(l, s, j, j_z|\mathbf{L}\cdot\mathbf{s}|l, s, j, j_z) &= \tfrac{1}{2}[j(j+1) - l(l+1) - s(s+1)]\,\hbar^2 \\ &= \begin{cases} \frac{1}{2}l\hbar^2 & \text{if } j = l + \frac{1}{2} \\ -\frac{1}{2}(l+1)\,\hbar^2 & \text{if } j = 1 - \frac{1}{2}. \end{cases}\end{aligned} \tag{5.18}$$

Thus the introduction of spin–orbit coupling splits the $(4l + 2)$-fold degenerate level (n, l) into two levels which we may label by $nl_{l+\frac{1}{2}}$, $nl_{l-\frac{1}{2}}$. For example, when $l = 2$ (d-states),

$$\text{nd (10 states)} \;\rightarrow\; \text{nd}_{\frac{5}{2}} \text{ (6 states) and } \text{nd}_{\frac{3}{2}} \text{ (4 states).}$$

Experiment shows that the sign of $U_{so}(r)$ is negative so that the state with $j = l + \frac{1}{2}$ always has lower energy than the state with $j = l - \frac{1}{2}$. Equation (5.18) suggests that the energy splitting increases with l, though of course the form of the radial function is also relevant in the calculation of the energy levels. The splitting is great enough to change the orbital sequence of columns (1) and (7) of Table 5.1. This effect is most apparent in the heavier nuclei, where because of increasing R the orbital levels are closer together in energy than in the lighter nuclei.

The sequence of 'shells' inferred from experiment is shown in columns (3) and (6) for neutrons and protons respectively. The shift of the proton

https://doi.org/10.1017/CBO9781139164405.008 Published online by Cambridge University Press

column relative to the neutron column reflects the shell filling observed for the β-stable nuclei. In the filling of these levels there are departures from the order given in the case of a few particular nuclei.

The major success of the shell model is the prediction of the angular momenta of nuclei in their ground states. These values follow simple rules: nuclei with an even number of protons and an even number of neutrons (even–even nuclei) have angular momentum zero and positive parity, nuclei with an even number of protons and an odd number of neutrons or vice-versa (even–odd nuclei), have angular momentum and parity equal to that of the odd nucleon in the shell that is being filled. We saw in Chapter 4 that it was energetically favourable for nuclei to contain even numbers of protons and even numbers of neutrons. The information from nuclear spins makes more precise the origin of this energy: it seems that it is energetically advantageous for nuclei to take pairs of protons and pairs of neutrons into the energy shells, with the angular momenta of the pairs coupled to zero, $\mathbf{J}_1 + \mathbf{J}_2 = 0$, so that the angular momentum and parity of an unpaired nucleon is the angular momentum and parity of the whole nucleus. There are some exceptions to this last rule, but remarkably few considering its simplicity.

In the case of odd–odd nuclei, the odd proton and odd neutron do not combine their angular momenta in any systematic way; there is no very clear empirical rule, and no simple theory. Indeed, odd–odd nuclei are altogether energetically disfavoured. There are only four stable odd–odd nuclei ($^2_1$H, $^6_3$Li, $^{10}_5$B, $^{14}_7$N), the rest undergo β-decay to become even–even (Chapter 4).

The rules may be seen obeyed by the light nuclei of Table 4.2. For example $^{17}_8$O has one odd neutron in the $1d_{\frac{5}{2}}$ shell, and spin and parity $\frac{5}{2}^+$.

5.4 Magic numbers

In Table 5.1 lines have been drawn where the total numbers of states in the shells above the line are 2, 8, 20, 28, 50, 82 and 126, the so-called 'magic numbers'. The first two numbers just correspond to the filling of 1s and 1p shells. The others appear to be somewhat arbitrary, but it is found empirically that the energy gaps to the next shell are greater than average at these points in the sequence. Nuclei having Z or N equal to one of these numbers have properties which reflect the existence of such a gap. For example, tin ($Z = 50$) has ten stable isotopes, and there are seven stable elements having $N = 82$ (see Fig. 4.6). These examples illustrate that there must be a large gap in the energy spacing at $Z = 50$ in the

https://doi.org/10.1017/CBO9781139164405.008 Published online by Cambridge University Press

proton sequence and at $N = 82$ in the neutron sequence, as is clear from our discussion in §5.2 of the condition $E_n^F \approx E_p^F$.

The departures from the smooth curve of binding energy per nucleon, given by the semi-empirical mass formula, are associated with the nuclear shell structure and the magic numbers. Magic number nuclei are particularly strongly bound and have been marked on Fig. 4.7. The heaviest α-stable nuclei are $^{208}_{82}$Pb, which is 'doubly magic' with $N = 126$, $Z = 82$, and $^{209}_{83}$Bi which has $N = 126$.

The magic numbers were identified experimentally before the shell model was established, and indeed the indications of shell structure provided by the existence of these numbers was a strong motivation for the formulation of the shell model. Other consequences of the magic numbers will be mentioned in the sections on the excited states of nuclei and atomic abundances in the Solar System.

5.5 The magnetic dipole moment of the nucleus

The successful description of nuclear angular momentum indicates the essential validity of the shell model. The model also gives a qualitative understanding of the magnetic dipole moments of nuclei. The magnetic moments of paired nucleons, like their spins, cancel exactly, and all even–even nuclei are found to have zero magnetic moments. A nucleus with angular momentum operator $\mathbf{J}$ (quantum numbers j, j_z) has a magnetic moment operator $\boldsymbol{\mu}$ which, averaged over the nucleons, must be aligned with $\mathbf{J}$, since $\mathbf{J}$ is the only vector available giving a preferred direction. The *magnetic dipole moment* $\boldsymbol{\mu}$ is defined by writing

$$\langle \boldsymbol{\mu} \rangle = \frac{\mu}{(j\hbar)} \langle \mathbf{J} \rangle, \tag{5.19}$$

where the brackets $\langle \cdots \rangle$ indicate any matrix element between the $(2j + 1)$ states labelled by j_z.

In a magnetic field $\mathbf{B} = (0, 0, B)$, which specifies the z-direction, the magnetic potential energy of the nucleus in the field is the expectation value of $-\boldsymbol{\mu} \cdot \mathbf{B} = -\mu_z B$. For a state of given j_z, this energy is, from equation (5.19),

$$E(j_z) = -\mu(j_z/j)B \tag{5.20}$$

https://doi.org/10.1017/CBO9781139164405.008 Published online by Cambridge University Press

so that there are $(2j+1)$ equally spaced energy levels corresponding to $j_z = -j, -j+1, \ldots, j$.

Transitions between these levels may be induced by a radio-frequency oscillating electromagnetic field of angular frequency ω where

$$\hbar\omega = |\mu|B/j. \tag{5.21}$$

Measurements of this resonance frequency in a known magnetic field give a precise value for the magnetic dipole moment. The phenomenon is called *nuclear magnetic resonance*, and has many applications in physics, chemistry and biology.

5.6 Calculation of the magnetic dipole moment

In our simple version of the shell model, the magnetic moment of an odd-A nucleus will arise entirely from the unpaired nucleon. If this unpaired nucleon is a proton, its orbital motion will give, as in classical magnetism, a moment

$$\boldsymbol{\mu}_L = \frac{e\mathbf{L}}{2m_\mathrm{p}} = \mu_\mathrm{N}\left(\frac{\mathbf{L}}{\hbar}\right), \tag{5.22}$$

where $\mu_\mathrm{N} = e\hbar/2m_\mathrm{p}$ is the *nuclear magneton*. A neutron, since it is uncharged, will give no orbital contribution.

To this must be added the intrinsic magnetic moment of the nucleon,

$$\boldsymbol{\mu}_\mathrm{s} = g_\mathrm{s}\mu_\mathrm{N}\left(\frac{\mathbf{s}}{\hbar}\right), \tag{5.23}$$

where (using the values quoted in equation (3.2)), $g_\mathrm{s} = 5.59$ for a proton and $g_\mathrm{s} = -3.83$ for a neutron.

Thus the total magnetic moment operator for a single nucleon is

$$\boldsymbol{\mu} = \boldsymbol{\mu}_L + \boldsymbol{\mu}_\mathrm{s} = \mu_\mathrm{N}[g_L\mathbf{L} + g_\mathrm{s}\mathbf{s}]/\hbar, \tag{5.24}$$

where $g_L = 1$ for a proton and $g_L = 0$ for a neutron. We can write this as

$$\boldsymbol{\mu} = \boldsymbol{\mu}_\mathrm{N}[\tfrac{1}{2}(g_L + g_\mathrm{s})(\mathbf{L}+\mathbf{s}) + \tfrac{1}{2}(g_L - g_\mathrm{s})(\mathbf{L}-\mathbf{s})]/\hbar,$$

and take the scalar product with $\mathbf{J} = \mathbf{L} + \mathbf{s}$ to give

https://doi.org/10.1017/CBO9781139164405.008 Published online by Cambridge University Press

$$\boldsymbol{\mu} \cdot \mathbf{J} = \mu_N[\tfrac{1}{2}(g_L + g_s)\mathbf{J}^2 + \tfrac{1}{2}(g_L - g_s)(\mathbf{L}^2 - \mathbf{s}^2)]/\hbar$$

(since $\mathbf{L}$ and $\mathbf{s}$ commute). Then the expectation value of each side of this equation for a state specified by (j, j_z, l, s) gives, using equation (5.19)

$$\left(\frac{\mu}{j}\right) j(j+1) = \mu_N[\tfrac{1}{2}(g_L + g_s)j(j+1) + \tfrac{1}{2}(g_L - g_s)(l(l+1) - s(s+1))]$$

so that

$$\mu = \mu_N\left[\frac{1}{2}(g_L + g_s)j + \frac{1}{2}(g_L - g_s)\frac{(l-s)(l+s+1)}{(j+1)}\right]. \tag{5.25}$$

Since $s = \frac{1}{2}$ and $j = l \pm \frac{1}{2}$ we finally obtain for the contribution from the upaired nucleon

$$\begin{aligned} \mu &= \mu_N[jg_L - \tfrac{1}{2}(g_L - g_s)] && \text{for } j = l + \tfrac{1}{2}, \\ \mu &= \mu_N\left[jg_L + \frac{j}{2(j+1)}(g_L - g_s)\right] && \text{for } j = l - \tfrac{1}{2}, \end{aligned} \tag{5.26}$$

which are referred to as the 'Schmidt values'.

These predictions of the simple model for a nucleus with an odd unpaired nucleon are not grossly wrong: almost all the observed magnetic moments for such nuclei lie between these two values. But they are not accurate predictions and there is no generally accepted explanation of the discrepancies. One possible reason is that the intrinsic magnetic moment of the nucleon is smaller in a nuclear environment than in free space. Another interpretation is that the magnetic moments provide a more sensitive test of the nuclear shell model than does the nuclear spin, and cooperative effects which we have neglected may contribute.

5.7 The electric quadrupole moment of the nucleus

Nuclei with spin $\geqslant 1$ usually have small permanent electric quadrupole moments. The size of this electric quadrupole moment gives an indication of the extent to which the distribution of charge (and hence matter) in the nucleus deviates from spherical symmetry. A nucleus is coupled through its electric quadrupole moment to the gradient, at the nuclear site, of the external electric field produced by the molecular or crystalline environment of the nucleus. Like the nuclear magnetic dipole moment, the

https://doi.org/10.1017/CBO9781139164405.008 Published online by Cambridge University Press

nuclear electric quadrupole moment provides a sensitive probe of this environment for chemistry and condensed matter physics.

Classically, the energy of a nuclear charge distribution $e\rho_{\mathrm{ch}}(\mathbf{r})$ in an external electrostatic potential $\phi(\mathbf{r})$ is

$$U = e\int \rho_{\mathrm{ch}}(\mathbf{r})\phi(\mathbf{r})\mathrm{d}^3\mathbf{r}.$$

We take the origin $\mathbf{r} = 0$ to be the centre of mass of the nucleus. Since $\rho_{\mathrm{ch}}(\mathbf{r})$ is confined to the small nuclear volume we can approximate $\phi(\mathbf{r})$ by the first few terms of a Taylor series,

$$\phi(\mathbf{r}) \approx \phi(0) - \mathbf{r}\cdot\mathbf{E} + \frac{1}{2}\sum_{i,j} x_i x_j \phi_{ij}, \tag{5.27}$$

where $\mathbf{E} = -\nabla\phi$ is the electric field, and

$$\phi_{ij} = \frac{\partial^2\phi}{\partial x_i \partial x_j} = -\frac{\partial E_i}{\partial x_j}, \quad \text{all evaluated at } \mathbf{r} = 0.$$

Here the indices i, j run from one to three, and we are using the notation $\mathbf{r} = (x_1, x_2, x_3)$, etc.

We then have

$$\mathrm{U} = e\mathbf{Z}\phi(0) - \mathbf{E}\cdot\mathbf{d} + \tfrac{1}{2}e\sum_{i,j}\phi_{ij}\int \rho_{\mathrm{ch}}(\mathbf{r})x_i x_j\,\mathrm{d}^3\mathbf{r},$$

where $\mathbf{d} = e\int \rho_{\mathrm{ch}}(\mathbf{r})\mathbf{r}\,\mathrm{d}^3\mathbf{r}$ is the electric dipole moment. The first term would be the energy if the nuclear charge Ze were a point charge at the origin. The second term is the electric dipole energy. Apart from negligible weak interaction effects, nuclear charge densities have the reflection symmetry $\rho_{\mathrm{ch}}(\mathbf{r}) = \rho_{\mathrm{ch}}(-\mathbf{r})$; thus nuclear electric dipole moments are zero, and the effects of the extended nuclear charge distribution appear in the term

$$\Delta U = \tfrac{1}{2}e\sum_{i,j}\phi_{ij}\int \rho_{\mathrm{ch}}(\mathbf{r})x_i x_j\,\mathrm{d}^3\mathbf{r},$$

which in general does not vanish.

https://doi.org/10.1017/CBO9781139164405.008 Published online by Cambridge University Press

If we neglect the charge density of atomic electrons at the nucleus, the external potential ϕ satisfies Laplace's equation

$$\nabla^2\phi = \sum_i \phi_{ij} = 0. \tag{5.28}$$

We can therefore re-write ΔU in the form

$$\Delta U = \frac{e}{6}\sum_{i,j} \phi_{ij} Q_{ij},$$

where

$$Q_{ij} = \int \rho_{\mathrm{ch}}(\mathbf{r})[3x_i x_j - \mathbf{r}^2\delta_{ij}]\mathrm{d}^3\mathbf{r}.$$

Q_{ij} is defined to be the *quadrupole moment tensor* of the classical charge distribution. δ_{ij} is the usual Kronecker δ. The additional term containing δ_{ij} does not change ΔU, because of (5.28), but makes $Q_{ij} \equiv 0$ if $\rho_{\mathrm{ch}}(\mathbf{r})$ is spherically symmetric.

Dimensional analysis suggests that for a nucleus which has a non-vanishing quadrupole moment

$$|Q_{ij}|/e \sim (\text{nuclear dimension})^2.$$

A nucleus in a neutral atom is subject to the electric field of the surrounding atomic electrons. The closed shells of inner atomic electrons will be distributed with near spherical symmetry, and will not contribute appreciably to a quadrupole field at the nucleus. Any quadrupole field will be produced by outer electrons, and it may therefore be anticipated that

$$\phi_{ij} \sim e/(4\pi\varepsilon_0)(\text{atomic dimension})^3.$$

Hence typically the interaction energy is of magnitude

$$\Delta U \sim \frac{e^2(\text{nuclear dimension})^2}{4\pi\varepsilon_0(\text{atomic dimension})^3} \sim 10^{-9}\ \text{eV}.$$

https://doi.org/10.1017/CBO9781139164405.008 Published online by Cambridge University Press

Such small energy shifts are detectable in radio-frequency spectroscopy, but it is clear that higher multi-pole moments arising from further terms in the Taylor expansion (5.27) will be unimportant.

The charge distribution in a nucleus must of course be treated quantum mechanically rather than classically, and we define the *electric quadrupole moment* operator by

$$Q_{ij} = \sum_{\text{protons } p} [3x_{pi}x_{pj} - \delta_{ij}\mathbf{r}_{\text{p}}^2],$$

where now the x_{pi} are the proton coordinates.

Just as the matrix elements of the (vector) magnetic dipole operator $\boldsymbol{\mu}$ are proportional to the matrix elements of the (vector) angular momentum operator $\mathbf{J}$, it can be shown that for the tensor operator Q_{ij}

$$\langle Q_{ij} \rangle = C\langle [\tfrac{3}{2}(J_iJ_j + J_jJ_i) - \delta_{ij}\mathbf{J}^2] \rangle,$$

where C is a constant, and again the brackets indicate any matrix elements between the $(2j + 1)$ nuclear states of angular momentum quantum number j, labelled by j_z. Thus all the matrix elements of Q_{ij} are determined by a single quantity. It is conventional to take the expectation value of Q_{33} in the state with j_z equal to its maximum value j, and define this as the *nuclear electric quadrupole moment* Q, so that

$$Q = C[3j^2 - j(j + 1)] = Cj(2j - 1),$$

or

$$C = \frac{Q}{j(2j - 1)}.$$

All other matrix elements are then determined in terms of Q. Note that Q vanishes for nuclei with $j = 0$ or $j = \frac{1}{2}$.

Experimental values of Q are obtained from spectral measurements on systems in which the field gradients can be accurately calculated. These values are often very much larger than, and sometimes differ in sign from, the predictions of the simple shell model. The implication is that the deformation of many nuclei from spherical symmetry is much larger than would be expected from the simple independent particle shell model. In reality the deformations must result from collective effects involving several nucleons. As might be expected, deviations from sphe-

https://doi.org/10.1017/CBO9781139164405.008 Published online by Cambridge University Press

rical symmetry are least in the neighbourhood of closed shells and largest for nuclei with shells which are around half-full.

Problems

5.1 In the model of §5.2, verify that when $N = Z = A/2$ then $E_n^F = E_p^F - \bar{U} \approx 38$ MeV.

5.2(*a*) Show that in the model of §5.2 the total kinetic energy of a nucleus containing N neutrons and Z protons is

$$[\tfrac{3}{5}NE_n^F + \tfrac{3}{5}Z(E_p^F - \bar{U})].$$

(*b*) For $(N - Z) \ll A$, this expression may be Taylor expanded about $N_0 = A/2$, $Z_0 = A/2$, $E_0^F \approx 38$ MeV. Show that

$$E_n^F \approx E_0^F\left[1 + \frac{2}{3}\frac{\Delta N}{N_0} - \frac{1}{9}\left(\frac{\Delta N}{N_0}\right)^2\right],$$

$$(E_p^F - \bar{U}) = E_0^F\left[1 - \frac{2}{3}\frac{\Delta N}{N_0} - \frac{1}{9}\left(\frac{\Delta N}{N_0}\right)^2\right],$$

where $\Delta N = -\Delta Z = (N - Z)/2$.

(*c*) Hence show that the total kinetic energy of the nucleons in the nucleus is approximately

$$\tfrac{3}{5}E_0^F A + \tfrac{1}{3}E_0^F\frac{(\mathrm{N} - \mathrm{Z})^2}{\mathrm{A}}$$

and therefore contributes ≈ -23 MeV to the coefficient '*a*' in the semi-empirical mass formula, and ≈ 13 MeV to the symmetry coefficient '*s*' (equation (4.5)).

5.3(*a*) Show from equation (5.1) that the average Coulomb energy of a proton in a nucleus of atomic number Z is

$$\bar{U}_c = \frac{6}{5}\frac{(Z-1)e^2}{4\pi\varepsilon_0 R}.$$

(*b*) Show that for $^{208}_{82}$Pb, $\bar{U}_c \approx 2\bar{U}$.

5.4 $^{40}_{20}$Ca is the heaviest stable nucleus with $Z = N$. (It is doubly magic.) The neutron separation energy is 15.6 MeV. Estimate the proton separation energy, and compare your estimate with the empirical value of 8.3 MeV.

5.5 Suggest values for the spins and parities of the following nuclei in their ground states:

$^{31}_{15}$P, $^{67}_{30}$Zn, $^{115}_{49}$In.

https://doi.org/10.1017/CBO9781139164405.008 Published online by Cambridge University Press

5.6 The measured spins, parities and magnetic moments of some nuclei are:

$$^{43}_{20}\mathrm{Ca}\left(\frac{7^-}{2}, -1.32\mu_\mathrm{N}\right), \quad ^{93}_{41}\mathrm{Nb}\left(\frac{9^+}{2}, 6.17\mu_\mathrm{N}\right), \quad ^{137}_{56}\mathrm{Ba}\left(\frac{3^+}{2}, 0.931\mu_\mathrm{N}\right),$$

$$^{197}_{79}\mathrm{Au}\left(\frac{3^+}{2}, 0.145\mu_\mathrm{N}\right), \quad ^{26}_{13}\mathrm{Al}(5^+, \text{not known}).$$

Compare these values with the predictions of the shell model.

5.7 Calculate the nuclear magnetic resonance frequencies for (*a*) protons, (*b*) $^{43}_{20}$Ca (see Problem 5.6), in a magnetic field of 1 tesla ($= 10^4$ gauss).

5.8 Show that for a uniformly charged ellipsoid of revolution

$$\frac{x^2 + y^2}{a^2} + \frac{z^2}{b^2} \leqslant 1,$$

of total charge Ze,

$$Q_{zz} = \tfrac{2}{5}Z(b^2 - a^2).$$

The nucleus $^{176}_{71}$Lu has $j = 7$ and a very large electric quadrupole moment of 8.0 barns. Suppose the nucleus in the state with $j_z = 7$ has approximately an ellipsoidal charge distribution of the form above. Calculate a and b.

https://doi.org/10.1017/CBO9781139164405.008 Published online by Cambridge University Press